Minireview

Benefits at the nanoscale: a review of nanoparticle-enabled processes favouring microbial growth and functionality

Muammar Mansor [1*] and Jie Xu[2]

[1]*Geomicrobiology, Center for Applied Geoscience, University of Tuebingen, Tuebingen, 72076, Germany.*
[2]*Department of Geological Sciences, the University of Texas at El Paso, El Paso, Texas, 79968.*

Summary

Nanoparticles are ubiquitous and co-occur with microbial life in every environment on Earth. Interactions between microbes and nanoparticles impact the biogeochemical cycles via accelerating various reaction rates and enabling biological processes at the smallest scales. Distinct from microbe-mineral interactions at large, microbe-nanoparticle interactions may involve higher levels of active recognition and utilization of the reactive, changeable, and thereby 'moldable' nano-sized inorganic phases by microbes, which has been given minimal attention in previous reviews. Here we have compiled the various cases of microbe-nanoparticle interactions with clear and potential benefits to the microbial cells and communities. Specifically, we discussed (i) the high bioavailabilities of nanoparticles due to increased specific surface areas and size-dependent solubility, with a focus on environmentally-relevant iron(III) (oxyhydr)oxides and pyrite, (ii) microbial utilization of nanoparticles as 'nano-tools' for electron transfer, chemotaxis, and storage units, and (iii) speculated benefits of precipitating 'moldable' nanoparticles in extracellular biomineralization. We further discussed emergent questions concerning cellular level responses to nanoparticle-associated cues, and the factors that affect nanoparticles' bioavailabilities beyond size-dependent effects. We end the review by proposing a framework towards more quantitative approaches and

by highlighting promising techniques to guide future research in this exciting field.

Introduction

Similar to microbes, nanoparticles (which are defined as clusters, crystals, and amorphous phases having at least one dimension of 1–100 nm, Caraballo *et al*., 2015), have been found prevalent and abundant in a wide range of natural systems, from groundwater, soils, volcanic ashes, glaciers, thawing permafrost, to lacustrine, riverine, estuarine and marine settings (Hochella *et al*., 2008; Gartman *et al*., 2014; Johnson *et al*., 2014; Tepe and Bau, 2014, 2015; Hirst *et al*., 2017; Graca *et al*., 2018; Hawkings *et al*., 2018; Schindler *et al*., 2019). In contrast to the consensus that microbial life is central to many geological and environmental processes on Earth, the integral role of nanoparticles in global biogeochemical cycles has only started to be recognized. The estimated total abundances of both nanoparticles and microbes on Earth are extremely high, at magnitudes of $>10^{27}$ (Hochella *et al*., 2019; converting from mass to number assuming reasonable molar mass and size) and $\sim 10^{30}$ (Kallmeyer *et al*., 2012), respectively. These gigantic numbers, combined with significant overlaps in the occurrence settings of nanoparticles and microbes, inevitably lead to enquiries of possible interplays between the two and effects of such interplays on the biogeochemistry of elements as well as on microbial physiology, evolution and ecology. Nanoparticles have been shown to be more reactive compared to larger mineral particles in numerous cases. This increased reactivity is a result of unique particle properties at the nanoscale, which include—but are not limited to—exceedingly high surface area-to-volume ratios, size- and shape-dependent solubilities, high surface energies, high densities of surface defects and strain, the wide range of atomic structural orders (i.e., crystallinity) and the high tendency of self-induced phase transformation and morphological changes (Banfield and Zhang, 2001; Gilbert *et al*., 2004; Misra

et al., 2012; Caraballo et al., 2015; De Yoreo et al., 2015). These properties of nanoparticles ultimately lead to their increased bioavailability and enhanced 'moldability', reflected in the preferential utilization of nanoparticles relative to larger particles by microbial life (see discussions in Sections 2 and 5).

While many studies on microbe-nanoparticle interactions were focused on the cytotoxic effects of engineered nanoparticles (i.e., metal oxides, silver, gold, quantum dots and carbon-based nanoparticles) released via anthropogenic activities (Hu et al., 2009; Kang et al., 2009; Priester et al., 2009; Aruguete et al., 2010; Aruguete and Hochella, 2010; Schacht et al., 2012; Xu et al., 2012; Sharma et al., 2014; Gil-Allué et al., 2018), recent studies have revealed that the presence of naturally-occurring nanoparticles may play important, if not essential, roles in enabling microbial metabolisms, with great benefits to single cells and to the overall microbial populations. In this review, we focus on compiling these beneficial interactions involving naturally-occurring nanoparticles, ranging from their high bioavailabilities, to their utilization by microbes as functional 'nano-tools" in assisting with electron transfer, chemotaxis, and substrate storage, as well as speculated roles in energy metabolism (Fig. 1). While many themes may be related and inherited from previous reviews on microbe-mineral interactions (Dong, 2010; Gadd, 2010; Benzerara et al., 2011; Miot et al., 2014; Shi et al., 2016), our focus here is specifically on the nanoscale phases and clusters and their distinctive roles from bulk minerals. Our compilation is not meant to be exhaustive; rather, it serves to highlight the diversity of beneficial microbe-nanoparticle interactions and to provide kernels upon which later environmental microbiological work may continue to build. We end the review by discussing current knowledge gaps in the field and possible directions for future investigations.

Nanoparticles as highly bioavailable nutrient sources: surface area effects and size-dependent dissolution

There are two main reasons as to why nanoparticles are more bioavailable compared to macro-particles (i.e., defined as larger particles with all dimensions of at least micron scales). First, the surface area-to-volume (SA/V) ratio of a particle is inversely proportional to the diameter of the sphere (Fig. 2A). As most microbial-particle interactions are governed by the effective surface area of contact, it is easy to see why nanoparticles are more bioavailable compared to macro-particles on the same per volume basis. Secondly, independent of the surface area, a mineral's solubility is also expected to
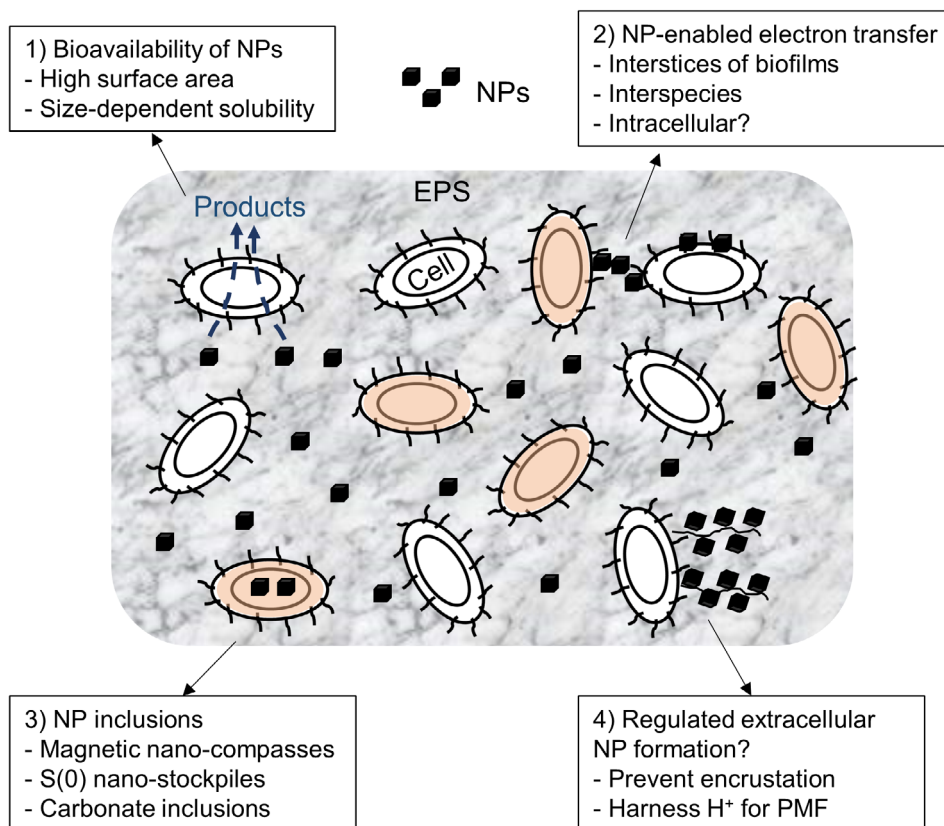

Fig 1. A summary of beneficial microbial-nanoparticle interactions in the environment. Different-coloured cells represent different species. Abbreviations: NPs (nanoparticles), EPS (Extracellular Polymeric Substances that constitute a biofilm), PMF (Proton Motive Force).
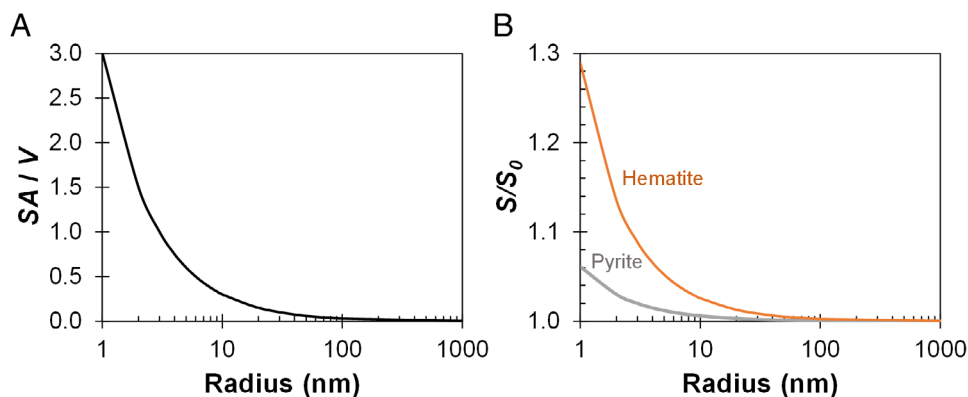
1) Bioavailability of NPs
- High surface area
- Size-dependent solubility

NPs

2) NP-enabled electron transfer
- Interstices of biofilms
- Interspecies
- Intracellular?

Products

EPS

Cell

3) NP inclusions
- Magnetic nano-compasses
- S(0) nano-stockpiles
- Carbonate inclusions

4) Regulated extracellular NP formation?
- Prevent encrustation
- Harness H$^+$ for PMF

A

B

Fig 2. The relationships of particle radius with (A) surface area-to-volume ratio (SA/V), assuming a spherical shape, and (B) the degree of solubility enhancement (S/S_0) of nano-hematite and nano-pyrite relative to the respective macro-particles. Parameters for hematite: γ = 10.375 J/m², V = 3.03 $\times$ 10⁻⁵ m³/mol; pyrite: γ = 3.072 J/m², V = 2.39 $\times$ 10⁻⁵ m³/mol (Robie and Bethke, 1966; Tromans and Meech, 2002).

increase exponentially with decreasing particle size according to the modified Kelvin equation: (Echigo et al., 2012):

$$S/S_0 = e^{2\gamma V/RTr} \tag{1}$$

Here, S is the solubility (mol/kg) of a mineral grain with a radius r (m), S_0 is the solubility of the bulk mineral, γ is the surface free energy (J/m²), V is the molar volume (m³/mol), R is the universal gas constant (J/mol/K) and T is the absolute temperature (K). Figure 2B exemplifies the size-dependent solubilities of two environmentally-relevant minerals: hematite (α-Fe$_2$O$_3$) and pyrite (FeS$_2$). Two observations are evident here: the solubilities are enhanced only when particle radii are reduced to below 100 nm, and further, the degree of solubility enhancement (S/S_0) depends on the mineral type, specifically on the mineral-specific parameters of γ and V. However, the solubility prediction can rarely be applied quantitatively, because surface free energies can vary as a factor of particle size and shape, solution chemistry, and the presence of structural impurities or defects (Banfield and Zhang, 2001; Tang et al., 2004; Wagner et al., 2014). Regardless, this relationship provides an additional basis for expecting higher bioavailability for nano- over macro-particles.

Two of the most commonly studied nanoparticles are iron(III)-(oxyhydr)oxides (Fe-oxides) and pyrite (FeS$_2$) due to the natural occurrence and the biogeochemical importance of these minerals throughout the Earth's near surface environments (Berner, 1984; Cornell and Schwertmann, 2003). Fe-oxides present a potentially rich source of Fe for incorporation into enzymes as reaction centers, or as electron acceptors for energy generation (Glass and Orphan, 2012; Melton et al., 2014; Bryce et al., 2018). Similarly, pyrite can be a rich source for Fe and sulphur (S) for protein building (e.g., disulphide bonds) or as electron donors for energy generation

(Jørgensen et al., 2019). Both of these minerals have low solubilities (Rickard and Luther, 2007); thus, the efficiency of microbial Fe- and S-related metabolisms depends greatly on the bioavailability of the solid phases.

In the case of Fe-oxides, multiple experimental studies have demonstrated that the bioavailability of Fe-oxides at circumneutral pH is dependent on their sizes. The growth rate of the aerobic bacterium *Pseudomonas mendocina* is 2 to 3 times faster in the presence of 9 nm versus 72 nm hematite under Fe-limited conditions (Dehner et al., 2011). Similarly, the Fe(III) reduction rates of *Geobacter sulfurreducens* and *Shewanella oneidensis* are 2 to 100 times faster in the presence of smaller-sized nano-hematite (Yan et al., 2008; Bose et al., 2009; Bosch et al., 2010). Interesting exceptions to the expected size-rate relationship are known in two cases however. First, the surface area-normalized reduction rates for nano-hematite by *G. sulfurreducens* appeared to follow the particle size order of 30 nm > 50 nm > 10 nm (Yan et al., 2008). Second, the surface area-normalized reduction rates by *S. oneidensis* appeared to be about 10× faster for the 99 nm compared to the ≤43 nm hematite (Bose et al., 2009). Thus, both of these studies demonstrated slower rates for the smaller nanoparticles in contrast to expectation. A follow-up study employing the purified Fe(III)-reducing enzyme OmcA isolated from *S. oneidensis* neatly demonstrated that these unexpected observations can be understood in terms of nanoparticle aggregation and pore throat sizes. Small nano-hematites aggregate closely together in solution, reducing the effective surface area that is accessible by the 'large' (∼10 × 6 × 5 nm) OmcA enzyme. In contrast, aggregates of larger nano-hematite are associated with larger pore throat sizes; thus, the effective surface area of the nanoparticles was not decreased, leading to an apparent faster Fe(III) production rate (Liu et al., 2016). This study highlights the importance in considering the structure and accessibility of aggregates compared to individual nanoparticles in microbial metabolisms. For

additional discussions on the importance of Fe-oxide nanoparticles in geomicrobiology and remediation, readers are referred to the excellent review by Braunschweig et al. (2013).

For pyrite, early studies were focused on aerobic pyrite oxidation at low pH because of the importance of this reaction in generating acid mine drainages. Pyrite oxidation and dissolution, mediated by microbial species such as *Acidithiobacillus*, can be up to 10^6 times faster compared to abiotic rates (reviewed by Gleisner et al., 2006). Both abiotic and microbial oxidation rates of pyrite were found to proportionally increase with decreasing particle sizes (Asai et al., 1992; Rimstidt and Vaughan, 2003). However, another study showed a more complex relationship between particle sizes and microbial oxidation rates of pyrite. While the oxidation rates were negatively correlated with particle sizes in the size range of 925–2830 μm, the rates were surprisingly positively correlated with particle sizes in the size range of 150–925 μm. It was suggested that this contrasting dissolution behaviour between different particle size ranges was due to variations in the defect densities on particle surfaces, which likely had an effect on bacterial attachment (Shrihari et al., 1995). We note here that only micron-sized pyrite particles have been examined in the aforementioned studies. The relevance and importance of nanoscale pyrite in acid mine drainages remain elusive to the best of our knowledge.

Only recently was it demonstrated that the oxidative dissolution of pyrite can be accelerated at circumneutral pH, depending on the microbial presence and pyrite particle sizes. Under aerobic conditions, the microbial oxidation rate for nano- to micron-sized pyrite was about ten times higher than abiotic controls, resulting in 30–50 nm thick ferrihydrite coatings on the pyrite's surface and the release of sulfate to the solution. Metagenomic analysis implicated the family *Bradyrhizobiacea* (*Alphaproteobacteria*) and the genus *Ralstonia* (*Betaproteobacteria*) for aerobic pyrite oxidation in that study (Percak-Dennett et al., 2017). Under anoxic conditions, the sulphur in pyrite (pyrite-S) can be oxidized with concurrent reduction of nitrate by *Thiobacillus denitrificans*, *Sulfurimonas* species, or by indigenous microbial communities in certain anoxic environments (Jørgensen et al., 2009; Bosch et al., 2011; Pu et al., 2014). These reactions were faster when smaller-sized pyrite particles were provided as the electron donor (Torrentó et al., 2010; Vaclavkova et al., 2015). Less than 9% of the pyrite-S was oxidized in each of these studies. The most recent study by Yan et al. (2018) highlighted the possibility that these previous studies may be misleading as bioavailable elemental sulphur (S^0) particles are common impurities associated with pyrite that was not pre-treated with organic solvents. Indeed, earlier studies found no pyrite oxidation when microbes were incubated in the presence of solvent-washed pyrite (Schippers and Jorgensen, 2002; Haaijer et al., 2007). Nevertheless, Yan et al. (2018) demonstrated that even with S^0 impurities in their experiments, about 4% of the pyrite-S must have been oxidized by *T. denitrificans* in order to explain the amount of sulfate produced. Overall, these studies demonstrated that the particle size of pyrite controls its bioavailability. As natural pyrite can vary in size from <100 nm to a few centimetres (Huang et al., 2017), these findings can have important implications to the biogeochemical cycling of Fe, S, oxygen and trace metals throughout Earth's history (Canfield, 2005; Johnston et al., 2009; Houben et al., 2017).

Besides Fe-oxides and pyrite, virtually all other minerals on Earth have a nanoparticulate component, generated either through weathering or during the earliest stages of nucleation and growth from a fluid. Field evidence of nanoparticles of silica, clays, carbonates, sulfates, halides, pure metals (e.g., silver, gold and copper) and non-metals (sulphur and selenium), and metal-rich oxides and sulfides was reviewed previously (Sharma et al., 2015; Griffin et al., 2018; Hochella et al., 2019). While these natural nanoparticles may occur in relatively high concentrations within certain localities depending on the geology, most of them remained to be examined with respect to their bioavailabilities and potential benefits to microbial activities. A few previous studies did examine the bioavailability of nanoscale to micron-sized iron-containing clays and manganese oxides as energy sources, and revealed that the microbial reduction rates of these substrates are largely controlled by the surface areas, morphology, and crystallinity of the minerals (Burdige et al., 1992; Kostka et al., 2002; Dong et al., 2003; Vorhies and Gaines, 2009; Pentráková et al., 2013; Novotnik et al., 2019).

Nanoparticle-assisted electron transfer among microbial cells

A key tenet of microbial energy metabolism involves the transfer of electrons from chemical species acting as electron donors to another species acting as electron acceptors. This poses a challenge when microbes live in micrometre-thick biofilms with limited accessibility to certain chemical species or when the electron donor and acceptor are spatially separated (e.g., sulfide and oxygen separated by a few centimetres within the sedimentary column). To overcome this problem, microbes are able to utilize conductive or semi-conductive nanoparticles (such as magnetite, hematite, graphite and mackinawite) as functional 'nano-tools" to assist in electron transfer (Kato et al, 2010; Jiang et al., 2014; Hu et al., 2018). Electron transfer from cell-to-cell or cell-to-macroparticles can be mediated by these nanoparticles either through direct

contact or indirectly through soluble organic mediators (Jiang *et al*., 2014). The addition of conductive nanoparticles to bacterial cultures was found to both increase biofilm thickness and to sustain greater cell viability throughout the different biofilm layers (Hu *et al*., 2018). While conductive macro-particles can also assist in electron transfer, the efficiency is likely less since only nanoparticles can form dense electrical conduits in the spaces within biofilms (Kato *et al*., 2010). There are tentative evidences that nanoparticles can even facilitate electron transfer in the periplasmic and intracellular space of microbes (Fu *et al*., 2019; Deng *et al*., 2020), due to the unique capability of extremely small nanoparticles (< 10 nm) to pass through the cell membrane (Kloepfer *et al*., 2005; Dehner *et al*., 2011).

Nanoparticles can also mediate electron transfer between species, resulting in coupling of metabolic pathways that would not have been otherwise possible (Liu *et al*., 2012; Kato *et al*., 2012b; Aulenta *et al*., 2013; Byrne *et al*., 2015; Tang *et al*., 2016; You *et al*., 2018). Nanoparticle-assisted electron transfer is particularly important for methanogenesis that relies on close interactions between *Bacteria* and *Archaea*; theoretical calculations indicate that interspecies electron flux via nanoparticles is about 10^6 times higher than using diffusible H_2 molecules (Cruz Viggi *et al*., 2014). Consistent with this calculation, methane-producing microbial communities enriched from paddy soils, anaerobic digesters and lake and coastal sediments display 0.3 to 4 times faster methane production rates when conductive nanoparticles are added to the cultures (Kato *et al*., 2012a; Yamada *et al*., 2015; Zhuang *et al*., 2015, 2018; Kato and Igarashi, 2018; Rotaru *et al*., 2018, 2019). In one particular case, methanogenesis was only sustainable in the presence of conductive nanoparticles (Rotaru *et al*., 2019). DNA analyses implicate *Geobacter* and *Methanosarcina* as the primary drivers for nanoparticle-assisted methanogenesis in most of these studies.

Another striking example of nanoparticle-assisted electron transfer is in the utilization of surface-bound nanoparticles by nonphotosynthetic bacteria to harvest electrons from visible light. Sakimoto *et al*. (2016) demonstrated that in the presence of cadmium sulfide (CdS) nanoparticles, the nonphotosynthetic bacterium *Moorella thermoacetica* can harness electrons from visible light-driven processes to form acetic acid from CO_2. Wang *et al*. (2017) applied a similar concept to *Escherichia coli*, resulting in enhanced rate of H_2 production by fermentation when the microbe-CdS hybrid were exposed to visible light. A series of recent studies (reviewed in Cestellos-Blanco *et al*., 2020) have further explored the idea of hybridizing photosensitive nanoparticles with microbial cells or cellular components for artificial photosynthesis. All of these are engineered systems designed to work in the laboratory however, with unclear relevance to natural systems. We speculate that metal clusters (e.g., manganese, nickel, copper, zinc and iron–sulphur complexes) utilized in modern photosynthetic electron transport (Raven *et al*., 1999) may have evolved from ancient interactions between microbes and metal-sulfide nanoparticles (likely discharged in high concentrations within terrestrial and shallow marine hydrothermal systems that are accessible to light), resonating with the theme of life origin and evolution in the metal-sulfide world (Beinert *et al*., 1997; Huber and Wächtershauser, 1998).

Beneficial nanoparticle inclusions

Due to their small sizes, nanoparticles can exist as inclusions within microbial cells. Some of these nanoparticles may be formed intracellularly as part of a detoxification mechanism (as reviewed in Hulkoti and Taranath, 2014) while nanoparticles <10 nm may be indiscriminately taken up by the cells from the extracellular solution due to their extremely small sizes (Kloepfer *et al*., 2005; Dehner *et al*., 2011). Here we focus on beneficial nanoparticle inclusions that are actively precipitated by the cells in order to serve specific metabolic functions (Fig. 3).

Magnetite/greigite inclusions in magnetotactic bacteria as nano-compasses

The discovery of magnetotactic bacteria represents the first ever report of microorganisms capable of utilizing nanoparticle inclusions for a specific metabolic function, in this case to enable navigation based on a magnetic field (Blakemore, 1975; Chen *et al*., 2010). The inclusions are composed of 30–140 nm single domain crystals of magnetite (Fe_3O_4) and/or greigite (Fe_3S_4) that are arranged in chains, causing the cells to align along the Earth's magnetic field lines (Faivre and Schueler, 2008). This helps the cells to navigate in habitats with vertical redox gradients as commonly found in their optimal environmental niches near the oxic-anoxic interface (Lefevre and Bazylinski, 2013). Magnetotactic bacteria are geographically and phylogenetically widespread, spanning the *Alphaproteobacteria*, *Deltaproteobacteria* and *Gammaproteobacteria* classes of the *Proteobacteria* phylum, the *Nitrospirae* phylum and the candidate phyla of *Omnitrophica* and *Latescibacteria* (Lin *et al*., 2017). Magnetotactic bacteria induce the formation of magnetite through solid-state transformation of precursor nanometric Fe(III)-oxides (similar to ferrihydrite; Baumgartner *et al*., 2013) or solid ferrous iron phases (similar to green rust; Baumgartner *et al*., 2016). Magnetotactic bacteria were recently found as symbionts of marine bivalves (Dufour *et al*., 2014) and protists (Monteil *et al*., 2019). It is speculated that endosymbiotic magnetotactic bacteria may
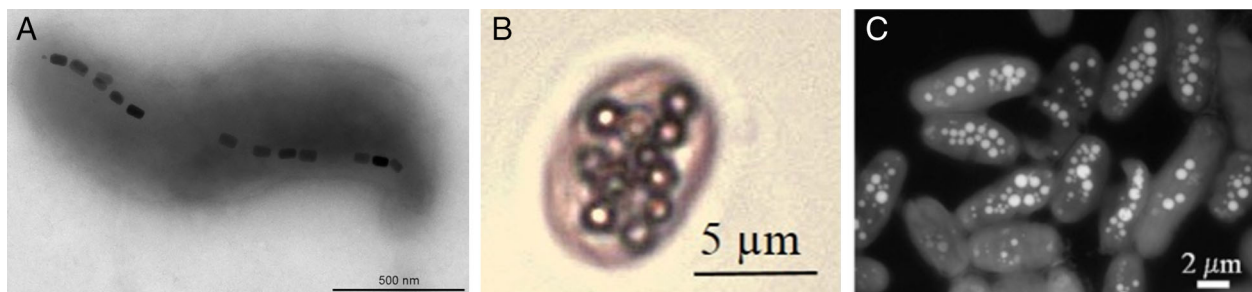
Fig 3. Microscopy images of nano-inclusions in microbes.
A. Magnetite in the magnetotactic bacterium *Magnetovibrio blakemorei* strain MV-1 (Abreu and Acosta-Avalos, 2018).
B. Elemental sulphur in the purple sulphur bacteria *Chromatium okenii* (Danza et al., 2017).
C. Nano-carbonate inclusions in the cyanobacterium *Cyanothece* sp. PCC 7425 (Benzerara et al., 2014).

contribute to the magnetic sensing capability of migrating animals, although this is yet to be proven (Natan and Vortman, 2017). The consistent morphology, size, and chemical purity of the magnetite/greigite nanoparticles formed within magnetotactic bacteria, along with the available technology to functionalize these nanoparticles' surface towards specific targets, renders the bacteria and their biogenic nanoparticles as potent candidates for applications in water remediation, food safety, drug delivery, magnetic resonance imaging and even for cancer treatment (Alphandéry, 2014; Ali et al., 2018; Vargas et al., 2018).

Elemental sulphur (S^0) inclusions in sulphur-oxidizing microbes as nano-stockpiles

Elemental sulphur inclusions can be formed intracellularly by a number of bacteria within the *Proteobacteria* phylum. These include small (≤ 5 μm) bacteria such as *Acidithiobacillus* (He et al., 2009), *Thiothrix* (Howarth et al., 1999) and green sulphur bacteria and purple sulphur bacteria (Gregersen et al., 2011), as well as the strikingly large (size up to 750 μm) members of the sulphur-oxidizing bacteria group such as *Beggiatoa*, *Thioploca*, *Thiomargarita*, *Thiovulum* and *Achromatium* (Dahl and Prange, 2006; Salman et al., 2011). These inclusions have a size range of 30 to ~2000 nm (Steudel, 1989; Findlay et al., 2014), with the larger inclusions likely being composed of amorphous to nano-crystalline aggregates of S^0 (Marnocha et al., 2019; Nims et al., 2019). The inclusions serve an important metabolic role by being a compact storage unit of S^0 to be used as reserve electron donors under low-nutrient conditions. The S^0 is accumulated under periods of high H_2S, reaching concentrations up to 1700 mM S^0 within a single cell (Schulz et al., 1999). When H_2S is depleted (e.g., during O_2-rich period), the S^0 inclusions can be oxidized to gain energy. This strategy confers metabolic flexibility to sulphur-oxidizing bacteria by allowing the cells to survive in environmental niches where electron donors and acceptors are spatially and temporally varied (e.g., Schulz et al., 1999). The S^0 inclusions may also be used as an electron acceptor coupled to the reduction of dihydrogen under anoxic conditions (Kreutzmann and Schulz-Vogt, 2016). Even though S^0 nanoparticles have various potential applications—such as antimicrobial and antifungal agents in medicinal, agricultural and food industry, as nutrient amendments in agriculture, and as components in lithium-sulphur batteries (Li et al., 2016; Shankar et al., 2020)—the utilization of microbial S^0 inclusions for these purposes is still underexplored.

Nano-carbonate inclusions in cyanobacteria: speculated functions

Recently, several species of cyanobacteria were discovered to harbour naturally-formed nanoscale carbonate inclusions; these cyanobacteria are geographically and phylogenetically widespread (Benzerara et al., 2014). Electron microscopy analysis indicated that the inclusions are 50–870 nm in size and are composed primarily of amorphous calcium (Ca) carbonate with varying amount of magnesium (Mg), barium (Ba) and strontium (Sr) (Couradeau et al., 2012; Benzerara et al., 2014; Cam et al., 2016). The inclusions make up 2%–4% of dry cell masses and can be formed even in the presence of extracellular solution undersaturated with respect to Ca-carbonate phases (Cam et al., 2018). Additionally, the inclusions display higher Sr/Ca and Ba/Ca ratios than the extracellular solution, indicating selective uptake of Sr and Ba during precipitation (Cam et al., 2016). These observations imply that the precipitation of the carbonate nanophases is actively mediated by the cells. Due to the discovery that the cells also selectively sequester radio-active Sr and radium over Ca, these cyanobacteria are touted as promising components of future bioremediation design for radioactive sites (Mehta et al., 2019).

Some cyanobacteria concentrate carbonate inclusions at the cell poles and septum, indicative of a link to the

intracellular Ca^{2+} regulation system during cell division (Benzerara *et al*., 2014). Others precipitate carbonate inclusions throughout the cytoplasm, and speculated functions of these inclusions include regulation of buoyant cell density, intracellular pH, inorganic carbon concentration (to optimize CO_2 fixation), or to regulate the saturation state of extracellular solution with respect to Ca-carbonates (to decrease the risk of cell encrustation) (Couradeau *et al*., 2012; Cam *et al*., 2018). Besides cyanobacteria, carbonate inclusions are also observed in the large sulphur bacteria from the genus *Achromatium*. Carbonate inclusions in *Achromatium* are larger (5–6 μm) and more crystalline (Gray and Head, 2014), and they are known to be formed within vesicles that are structurally different than those in cyanobacteria (Blondeau *et al*., 2018). It is interesting to consider if the ability to form carbonate inclusions is an example of convergent evolution in these two separate microbial lineages. Additional speculated functions for carbonate inclusions in *Achromatium* are as storage units for inorganic carbon for CO_2 fixation (Babenzien, 1991; Head *et al*., 1995) and as a harnessable proton source derived from the proton-releasing precipitation reaction (Mansor *et al*., 2015).

Nanoparticle-based processes in extracellular biomineralization: easier control and moldability?

While the ability to precipitate intracellular nanoparticles is restricted to specific microbial species, many different microbial populations are known to mediate extracellular biomineralization. Widespread extracellular biomineralization results from the modification of the bulk solution chemistry through microbial metabolisms and have important implications to natural biogeochemical cycling, environmental remediation, and industrial applications. Examples of extracellular biomineralization are induced calcite formation via alkalinity generated from oxygenic photosynthesis (Dupraz *et al*., 2009), Fe-oxide formation via Fe^{3+} from Fe(II)-oxidizing microbes (Chan *et al*., 2011; Posth *et al*., 2014), manganese-oxide formation from Mn(II)-oxidizing microbes (Wright *et al*., 2016), metal sulfide formation via sulfide (H_2S) from sulfate-reducing microbes (Moreau *et al*., 2004; Picard *et al*., 2016; Thiel *et al*., 2019) and gypsum formation via sulfate from S-oxidizing microbes (Harouaka *et al*., 2016). Mineral precipitation prevents accumulation of toxic metabolic products (e.g., H_2S) and also maintains the thermodynamic potential of the metabolic reaction so as to support optimal growth (Amend and LaRowe, 2019; Labrado *et al*., 2019). As all minerals go through a nanoparticle stage during formation, (Hochella *et al*., 2008), there is ample opportunity for microbes to influence the early stages of extracellular biomineralization. The formed nanoparticles can either remain as nanoparticles as

terminal products (e.g., ferrihydrite) or grow into macroparticles through a combination of dissolution-precipitation, ion attachment, and/or nanoparticle attachment processes that can be modulated by the presence of organics (De Yoreo *et al*., 2015). One of the major questions for extracellular biomineralization is: to what extent is the process regulated by the microbes versus being simply a fortunate side-process? Here, we will discuss how a nanoparticle-based perspective can help us to evaluate the extent of microbial regulation, focusing on the potential benefit of extracellular biomineralization to ATP generation.

Since some mineral formation is accompanied by the release of protons (H^+) (Equation 2–3), any microbes that can harness the released H^+ to supplement the proton motive force for ATP generation may have an additional advantage in the environment.

$$Fe^{3+} + 2H_2O \rightarrow FeOOH_{(m)} + 3H^+ \qquad (2)$$

$$Fe^{2+} + H_2S/HS^- \rightarrow FeS_{(m)} + 2H^+/H^+ \qquad (3)$$
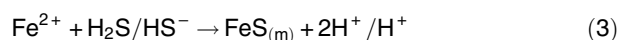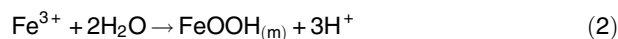
There are two key considerations here however to make such a pathway feasible: (i) the mineralization process needs to occur closely associated with microbial cell membranes to render the released protons usable, and (ii) the mineralization products should not cut off the continuity of this process. Fe(II)-oxidizing bacteria seem to have evolved a perfect solution for this by producing micrometre-long filaments as organic templates for the formation of Fe-oxide nanoparticles and for their assembly into 'stalk' structures (Fig. 4). The production of these filaments potentially play a dual role in preventing cell encrustation and to direct mineralization near the cells where the released H^+ can still be harnessed (Chan *et al*., 2004). The cell surfaces themselves are associated with a near-neutral charge that inhibits precipitation directly on the cell membrane, thus preventing encrustation and favouring precipitation on the filaments (Saini and Chan, 2013). Involving nanoparticles, to some extent, enhances the feasibility of the hypothesized strategy because of the small sizes of primary biomineral nanoparticles and their flexibility in organization along the stalks.

Besides evolving specialized organic templates, microbes may also harness H^+ from nanoparticles that directly form on the cell walls, such as the case for Fe-oxides on the cells walls of some Fe-oxidizing bacteria (Miot *et al*., 2009) and Fe-sulfides on sulfate-reducing bacteria (Picard *et al*., 2018; Stanley and Southam, 2018; Mansor *et al*., 2019a), respectively. The microbes in these cases need to delicately balance potential benefits versus the risk of cell encrustation and death (Miot *et al*., 2015). The combined modification of the cells' surfaces, secreted organic molecules and the chemistry of
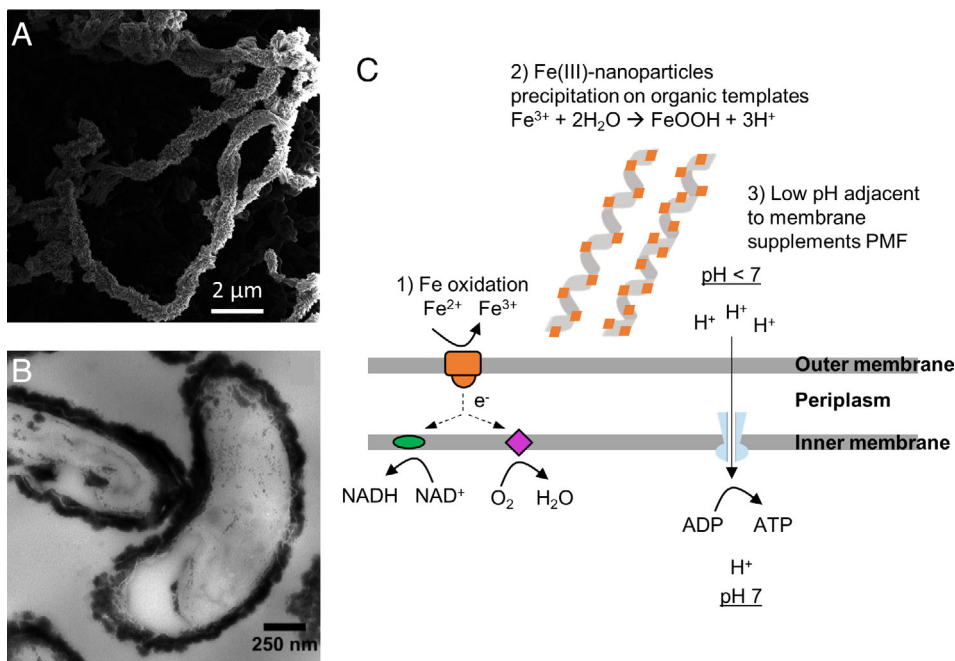
Fig 4. A. Microscopy image of filamentous Fe(II)-oxidizers as an example of directed nanoparticle formation via organic templates. Courtesy of James Byrne, University of Bristol.
B. Microscopy image of FeS-covered sulfate-reducing bacteria (Picard et al., 2018).
C. Schematic of the proposed mechanism by which a microbe may be able to direct nanoparticle precipitation and harness the released H^+ for maintenance of the proton motive force (PMF) across cell membrane (based on Chan et al. (2004) and Garber et al. (2020). Similar mechanisms could apply to any nanoparticle formation that releases H^+ during precipitation.

the cell microenvironments may allow some measure of regulation to prevent cell encrustation, primarily by affecting nanoparticle growth, dissolution and adsorption reactions. Secretion of organic molecules and protons can encourage dissolution of the nanoparticle crust by forming metal–ligand complexes and modifying the saturation state of the minerals (e.g., Fortin *et al*., 1994; Hegler *et al*., 2010; Lazo *et al*., 2017). Soluble organic molecules can also affect the morphology, size and crystallinity of minerals, with the exact effects dependent on the identity of the organic molecules and the minerals being studied (Xu *et al*., 2016; Harouaka *et al*., 2017; Mansor *et al*., 2020). Stabilization of the nanoparticles at their small sizes may allow encapsulation by membrane vesicles that can then be exported away from the cell walls (Shao *et al*., 2014). On the other hand, binding of metals to the cell walls combined with active pumping of protons generates localized microenvironments that are proposed to accelerate nanoparticle growth compared to those in the bulk solution (Picard *et al*., 2018; Mansor *et al*., 2019a, 2019b). This may form larger minerals that are more easily 'shed' from the cell walls compared to nanoparticles. However, the recent finding that soluble organics harvested from *E. coli* are just as potent at inducing extracellular S^0 formation compared to organics from the S-oxidizing bacteria *Sulfuricurvum kujiense* (Cron *et al*., 2019) indicates a non-specific role of organic molecules in directing mineralization. The delicate balance between nanoparticle (trans)formation and microbial responses needs to be understood in order to better determine the extent of regulation that microbes have in directing extracellular biomineralization. In this respect, (meta)omics-based approaches (including genomics, transcriptomics and proteomics) will likely be an important contributor to future studies.

Future directions

Despite the significant progress achieved in microbe-nanoparticle research in recent years, we have identified several aspects that remain understudied. The major ones include microbe-nanoparticle interaction mechanism at the cellular level, consideration of nano-scale effects beyond size, approaches in quantifying nanoparticle-mediated biological process in elemental cycling, and development of tools to track the morphological and biochemical changes of microbe-nanoparticle assemblages *in situ*, as respectively discussed below.

Microbe-nanoparticle interaction mechanisms at the cellular level

One of the most fundamental gaps in microbe-nanoparticle interaction research concerns if microbial cells may 'recognize' nanoparticles as a distinctive form of environmental cues from soluble ions or bulk surfaces. In other words, how the exposure to nanoparticles and subsequent microbe-nanoparticle interactions may modify microbial cells' gene regulation and expression remains largely elusive, except for studies focusing on the cytotoxic effects of engineered nanoparticles towards

pure cultures (i.e., microalgae, bacteria and yeasts) and model microbial communities (Monrás *et al*., 2014; Lagarde *et al*., 2016; Revel *et al*., 2017; Déniel *et al*., 2019; Horstmann *et al*., 2019; Singh, 2019). Within these studies, a few representative cases suggest that microbial cells respond to nanoparticle-specific cues at the genetic level. For example, *Pseudomonas aeruginosa* differentially expressed ∼28% and ∼ 43% of their total transcripts in response to silver nanoparticles and silver ions, respectively, compared to untreated samples (Singh *et al*., 2019). These genes are mainly involved in cell adhesion and dispersion, and also curiously in alkane degradation and denitrification. Transcriptomic profiling of the model microalgae *Chlamydomonas reinhardtii* also suggested recognition of different nanoparticles. Specifically, a decrease at the transcript level linked with photosynthesis was identified for *C. reinhardtii* exposed to TiO_2 or ZnO nanoparticles whereas an increase of gene transcripts linked to biosynthesis of proteasome and cell wall components was observed for cells exposed to silver nanoparticles (Simon *et al*., 2013). Further, a recent study examined the effects of gold nanoparticles with various morphologies and coatings on the taxonomy and functional gene expressions of model microbial communities from wastewater treatment reactors. It was found that the morphology of the gold nanoparticles has a more dominant influence over the microbial community structure and the abundances of antibiotic- and metal-resistance genes compared to the nanoparticles' surface coatings (Metch *et al*., 2018). Finally, addition of hydroxyapatite particles with different sizes to soils were found to influence microbial community in a complex manner, suggesting size-dependent responses (Cui *et al*., 2018). Genetic manipulation (i.e., creating knock-out mutant strains) has also been used in studies on electron transfer between microbes and nanoparticles. For example, *Geobacter sulfurreducens* was demonstrated to express different pathways for energy harvesting depending on the aging treatment of the Fe-oxide substrates, even when the aging treatment was shown to not generate any discernible changes in the X-ray diffraction patterns of the minerals (Levar *et al*., 2017). Using transcriptomic and proteomic tools to interpret microbe-nanoparticle interaction mechanisms is not trivial, but the fast development of these high-throughput methods into more easily accessible and understandable components is certain to drive new breakthroughs, especially with respect to microbial regulation of nanoparticle (trans) formation.

Beyond size-dependent effects

There is a need to broaden our view on the factors controlling the bioavailability of nanoparticles in natural environments, from the well-studied importance of surface area and size-dependent solubility, to the less explored effects of surface coating, particle shapes, surface charges, structural defects, and aggregation. In the case of the S-oxidizing bacteria *Chlorobaculum tepidum*, the organic coating of extracellular S^0 strongly affects its bioavailability (Marnocha *et al*., 2019). Different shapes of the same nanoparticle can induce differing microbial responses, which is hypothesized to be associated with the specificity of microbe-nanoparticle surface recognition as well as the relative amount of high-reactivity mineral surfaces (Pal *et al*., 2007; Metch *et al*., 2018). Shape, size, and surface coating of (nano)particles were also shown to affect binding of the particles to *E. coli* and *Helicobacter pylori* (Westmeier *et al*., 2018). Reaction rates are controlled by the density of defects on the surface, which can lead to higher reaction rates for defect-rich nanoparticles compared to defect-poor nanoparticles (Eskelsen *et al*., 2018). Lastly, it has been suggested that the binding efficiency of the same nanoparticle to microbes may differ depending on the bacterial species (discussed in Stauber *et al*., 2018) and the bacterial growth state (Eymard-Vernain *et al*., 2018). Since most of these studies employed engineered nanoparticles, we suggest that similar studies can be designed with a focus on microbial interactions with natural nanoparticles or their synthetic analogues.

Besides the characteristics of individual nanoparticles, future studies should also consider the impact of aggregation on microbe-nanoparticle interactions. Homo-aggregation (aggregation of particles of similar size, shape and elemental composition) has been shown to lead to lower surface areas and lower abiotic dissolution rates (Liu *et al*., 2009; Echigo *et al*., 2012), but there is also a need to consider heteroaggregation (aggregation of particles of different sizes, shapes and elemental compositions) processes that are most likely more important in the environment (Hotze *et al*., 2010). Heteroaggregation of ferrihydrite with biochar or clay minerals modified the microbial Fe(III) reduction rate depending on the exact composition of the heteroaggregates (Yang *et al*., 2020; Zeng *et al*., 2020). The process of aggregation is also impacted by the nanoparticles' size, shape, and surface coating, leading to a potentially complex interplay between all these parameters (Hotze *et al*., 2010).

Towards quantitative approaches in evaluating nanoparticle importance in nature

Microbially-mediated elemental cycling via nanoparticles has been repeatedly proposed to be important in a wide variety of environments, but quantitative description of their importance is lacking. Observations for the presence of nanoparticles do not automatically means that the said nanoparticles are important. An important question to
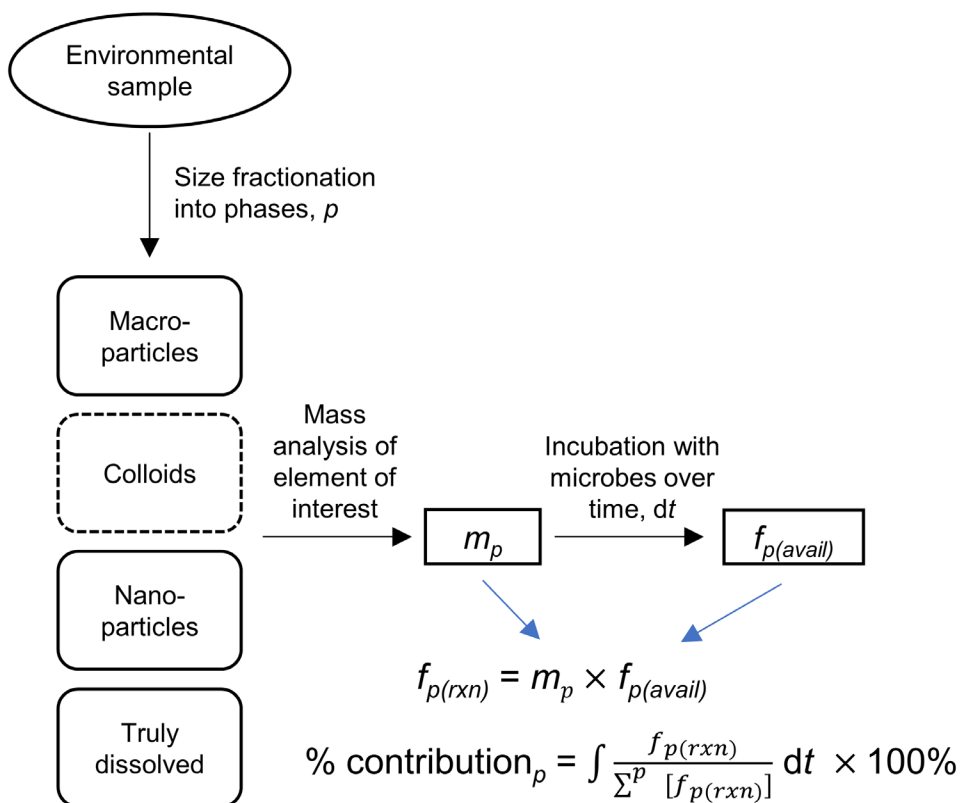
consider in any system of interest is the relative involvement of the dissolved, nanoparticulate, and macroparticulate phases in microbial reactions (Fig. 5). The following equations may be used to conceptually describe the relative contribution of the various phases to a particular reaction:

$$f_{p(rxn)} = m_p \times f_{p(avail)} \qquad (4)$$

$$\%\text{contribution}_p = \int \frac{f_{p(rxn)}}{\sum\limits^{p} [f_{p(rxn)}]} \, dt \times 100\% \qquad (5)$$

Here, the subscript 'p' stands for one of the three described phases (dissolved, nanoparticles or macro-particles), $f_{p(rxn)}$ stands for the fraction of the specified phase that is involved in a given reaction, m_p is the mass of a given element within the specified phase, $f_{p(avail)}$ is the fraction of mass within a specified phase that is actually (bio)available, and t stands for time. The value of $f_{(avail)}$ should theoretically approach unity for the dissolved and nanoparticulate phases, while it may be significantly less for macroparticles. For nanoparticles, the values of $f_{(avail)}$ may not only be a function of size, but also of aggregation state, shape and surface coatings, and our assumption of a value approaching unity for $f_{(avail)}$ warrants further testing under conditions specific to the system of

interest. With these equations, and a good handle of the mass balance of the whole system, it thus becomes possible to conceptualize the relative contribution of nanoparticles, compared to the dissolved and macroparticulate phases, for any given reaction. The inclusion of dt is an attempt to incorporate kinetics into consideration, which is important in evaluating the involvement of dynamic nanoparticles. Over short time scales, we expect processes involving the more bioavailable dissolved and nanoparticulate phases to be important. Over longer time scales, processes involving the macroparticles (that can often dominate the mass of a given system) may be more important. The parameter dt is therefore a function of the incubation time in laboratory experiments or residence time in the environment. The whole reaction can be made more accurate by incorporating kinetics (as rate, R) and thermodynamics (as solubility, S and surface free energy, γ) factors, as well as the important yet complex cascading effects in which dissolving macroparticles (either primarily macro-sized or of aggregated nanoparticles) are continuously evolving into smaller particles, and dissolving particles into dissolved ions. It is also important to note that while we consider nanoparticles in this review to be those in the 1–100 nm size range, the equations are also applicable for operationally-defined 'nanoparticles" in the 1–220 nm or 1–450 nm size range that are primarily based on common

pore sizes of commercially-available filters. In some systems, it may also be of interest to differentiate colloids (particles smaller than 1000 nm in at least one dimension; Caraballo *et al*., 2015) from nanoparticles and larger-sized macro-particles.

Application of new analytical tools

Our understanding on microbe-nanoparticle interactions will likely be accelerated in the near future with the increasing availability of state-of-the-art techniques such as liquid cell transmission electron microscopy (LCTEM), cryogenic electron microscopy, and single-particle inductively coupled plasma mass spectrometry (spICP-MS). LCTEM has been used to provide 2D imaging of nanoparticles *in situ*, allowing for direct measurements of nanoparticle dissolution rates as a function of aggregate size and compactness (Li *et al*., 2019). Cryogenic electron tomography (cryo-ET) using transmission electron microscopy has provided incredibly detailed images of the 3D fractal structure of Fe-oxide aggregates, thus directly linking aggregate structure to transport properties (Legg *et al*., 2014a, 2014b). Similarly, cryogenic-focused ion beam-scanning electron microscopy (cryo-FIB-SEM) will soon provide 3D structures of microbial-nanoparticle aggregates. Lastly, spICP-MS can provide the elemental compositions of hundreds to thousands of suspended nanoparticle aggregates within minutes (Lee *et al*., 2014; Bevers et al., 2020). A derivation of this technique has already been used to probe the variation in Fe content of magnetotactic bacteria at the single cell levels using single-cell ICP-MS (Amor *et al*., 2020). All of these techniques will be capable of probing microbe-nanoparticle interactions at an unprecedented scale. Overall, the environmental prevalence and multiple feedbacks involved in microbe-nanoparticle interactions lend this as one of the most exciting research fields for the next few decades.

Acknowledgements

References

Abreu, F., and Acosta-Avalos, D. (2018) Biology and physics of magnetotactic bacteria. In *Metagenomics-Basics, Methods and Applications*, England: IntechOpen, pp. 1–19.

Ali, I., Peng, C., Khan, Z.M., Naz, I., and Sultan, M. (2018) An overview of heavy metal removal from wastewater using magnetotactic bacteria. *J Chem Technol Biotechnol* **93**: 2817–2832.

Alphandéry, E. (2014) Applications of magnetosomes synthesized by magnetotactic bacteria in medicine. *Front Bioeng Biotechnol* **2**: 1–6.

Amend, J.P., and LaRowe, D.E. (2019) Minireview: demystifying microbial reaction energetics. *Environ Microbiol* **21**: 3539–3547.

Amor, M., Tharaud, M., Gélabert, A., and Komeili, A. (2020) Single-cell determination of iron content in magnetotactic bacteria: implications for the iron biogeochemical cycle. *Environ Microbiol* **22**: 823–831.

Aruguete, D.M., and Hochella, M.F. (2010) Bacteria-nanoparticle interactions and their environmental implications. *Environ Chem* **7**: 3–9.

Aruguete, D.M., Guest, J.S., Yu, W.W., Love, N.G., and Hochella, M.F. (2010) Interaction of CdSe/CdS core-shell quantum dots and *Pseudomonas aeruginosa*. *Environ Chem* **7**: 28–35.

Asai, S., Konishi, Y., and Yoshida, K. (1992) Kinetic model for batch bacterial dissolution of pyrite particles by *Thiobacillus ferrooxidans*. *Chem Eng Sci* **47**: 133–139.

Aulenta, F., Rossetti, S., Amalfitano, S., Majone, M., and Tandoi, V. (2013) Conductive magnetite nanoparticles accelerate the microbial reductive dechlorination of trichloroethene by promoting interspecies electron transfer processes. *ChemSusChem* **6**: 433–436.

Babenzien, H.-D. (1991) *Achromatium oxaliferum* and its ecological niche. *Zentralbl Mikrobiol* **146**: 41–49.

Banfield, J.F., and Zhang, H. (2001) Nanoparticles in the environment. *Rev Mineral Geochemistry* **44**: 1–158.

Baumgartner, J., Morin, G., Menguy, N., Gonzalez, T.P., Widdrat, M., Cosmidis, J., and Faivre, D. (2013) Magnetotactic bacteria form magnetite from a phosphate-rich ferric hydroxide via nanometric ferric (oxyhydr)oxide intermediates. *Proc Natl Acad Sci U S A* **110**: 14883–14888.

Baumgartner, J., Menguy, N., Gonzalez, T.P., Morin, G., Widdrat, M., and Faivre, D. (2016) Elongated magnetite nanoparticle formation from a solid ferrous precursor in a magnetotactic bacterium. *J R Soc Interface* **13**: 20160665.

Beinert, H., Holm, R.H., and Münck, E. (1997) Iron-sulfur clusters: nature's modular, multipurpose structures. *Science (80-)* **277**: 653–659.

Benzerara, K., Miot, J., Morin, G., Ona-Nguema, G., Skouri-Panet, F., and Férard, C. (2011) Significance, mechanisms and environmental implications of microbial biomineralization. *Comptes Rendus — Geosci* **343**: 160–167.

Benzerara, K., Skouri-Panet, F., Li, J., Ferard, C., Gugger, M., Laurent, T., *et al*. (2014) Intracellular calcium carbonate biomineralization is widespread in cyanobacteria. *Proc Natl Acad Sci*, **111**: 10933–10938.

Berner, R.A. (1984) Sedimentary pyrite formation: an update. *Geochim Cosmochim Acta* **48**: 605–615.

Bevers, S., Montaño, M.D., Rybicki, L., Hofmann, T., von der Kammer, F., Ranville, J.F. (2020). Quantification and characterization of nanoparticulate zinc in an urban watershed. *Frontiers in Environmental Science*, **8**: 84. http://dx.doi.org/10.3389/fenvs.2020.00084.

Blakemore, R.P. (1975) Magnetotactic bacteria. *Science (80-)* **4221**: 377–379.

Blondeau, M., Sachse, M., Boulogne, C., Gillet, C., Guigner, J. M., Skouri-Panet, F., *et al*. (2018) Amorphous calcium carbonate granules form within an intracellular compartment in calcifying cyanobacteria. *Front Microbiol* **9**: 1–14.

Bosch, J., Heister, K., Hofmann, T., and Meckenstock, R.U. (2010) Nanosized iron oxide colloids strongly enhance microbial iron reduction. *Appl Environ Microbiol* **76**: 184–189.

Bosch, J., Lee, K.Y., Jordan, G., Kim, K.-W., and Meckenstock, R.U. (2011) Anaerobic, nitrate-dependent oxidation of pyrite nanoparticles by *Thiobacillus denitrificans*. *Environ Sci Technol* **46**: 2095–2101.

Bose, S., Hochella, M.F., Gorby, Y.A., Kennedy, D.W., McCready, D.E., Madden, A.S., and Lower, B.H. (2009) Bioreduction of hematite nanoparticles by the dissimilatory iron reducing bacterium *Shewanella oneidensis MR-1*. *Geochim Cosmochim Acta* **73**: 962–976.

Braunschweig, J., Bosch, J., and Meckenstock, R.U. (2013) Iron oxide nanoparticles in geomicrobiology: from biogeochemistry to bioremediation. *N Biotechnol* **30**: 793–802.

Bryce, C., Blackwell, N., Schmidt, C., Otte, J., Huang, Y.M., Kleindienst, S., *et al* (2018) Microbial anaerobic Fe(II) oxidation—ecology, mechanisms and environmental implications. *Environ Microbiol* **20**: 3462–3483.

Burdige, D.J., Dhakar, S.P., and Nealson, K.H. (1992) Effects of manganese oxide mineralogy on microbial and chemical manganese reduction. *Geomicrobiol J* **10**: 27–48.

Byrne, J.M., Klueglein, N., Pearce, C., Rosso, K.M., Appel, E., and Kappler, A. (2015) Redox cycling of Fe(II) and Fe(III) in magnetite by Fe-metabolizing bacteria. *Science (80-)* **347**: 1473–1476.

Cam, N., Benzerara, K., Georgelin, T., Jaber, M., Lambert, J. F., Poinsot, M., *et al*. (2016) Selective uptake of alkaline earth metals by cyanobacteria forming intracellular carbonates. *Environ Sci Technol* **50**: 11654–11662.

Cam, N., Benzerara, K., Georgelin, T., Jaber, M., Lambert, J. F., Poinsot, M., *et al*. (2018) Cyanobacterial formation of intracellular ca-carbonates in undersaturated solutions. *Geobiology* **16**: 49–61.

Canfield, D.E. (2005) The early history of atmospheric oxygen: homage to Robert M. Garrels. *Annu Rev Earth Planet Sci* **33**: 1–36.

Caraballo, M.A., Michel, F.M., and Hochella, M.F. (2015) The rapid expansion of environmental mineralogy in unconventional ways: beyond the accepted definition of a mineral, the latest technology, and using nature as our guide. *Am Mineral* **100**: 14–25.

Cestellos-Blanco, S., Zhang, H., Kim, J.M., Shen, Y.X., and Yang, P. (2020) Photosynthetic semiconductor biohybrids for solar-driven biocatalysis. *Nat Catal* **3**: 245–255.

Chan, C.S., De Stasio, G., Welch, S.A., Girasole, M., Frazer, B.H., Nesterova, M.V., *et al* (2004) Microbial polysaccharides template assembly of nanocrystal fibers. *Science (80-)* **303**: 1656–1658.

Chan, C.S., Fakra, S.C., Emerson, D., Fleming, E.J., and Edwards, K.J. (2011) Lithotrophic iron-oxidizing bacteria produce organic stalks to control mineral growth: implications for biosignature formation. *ISME J* **5**: 717–727.

Chen, L., Bazylinski, D.A., and Lower, B.H. (2010) Bacteria that synthesize nano-sized compasses to navigate using Earth's geomagnetic field. *Nat Educ Knowl* **3**: 30.

Cornell, R.M., and Schwertmann, U. (2003) *The Iron Oxides: Structure, Properties, Reactions, Occurrences and Uses*. Weinheim, Germany: John Wiley & Sons.

Couradeau, E., Benzerara, K., Gerard, E., Moreira, D., Bernard, S., Brown, G.E., and Lopez-Garcia, P. (2012) An early-branching microbialite cyanobacterium forms intracellular carbonates. *Science (80-)* **336**: 459–462.

Cron, B., Henri, P., Chan, C.S., Macalady, J.L., and Cosmidis, J. (2019) Elemental sulfur formation by *Sulfuricurvum kujiense* is mediated by extracellular organic compounds. *Front Microbiol* **10**: 2710.

Cruz Viggi, C., Rossetti, S., Fazi, S., Paiano, P., Majone, M., and Aulenta, F. (2014) Magnetite particles triggering a faster and more robust syntrophic pathway of methanogenic propionate degradation. *Environ Sci Technol* **48**: 7536–7543.

Cui, H., Shi, Y., Zhou, J., Chu, H., Cang, L., and Zhou, D. (2018) Effect of different grain sizes of hydroxyapatite on soil heavy metal bioavailability and microbial community composition. *Agric Ecosyst Environ* **267**: 165–173.

Dahl, C., and Prange, A. (2006) Bacterial sulfur globules: occurrence , structure and metabolism. In *Inclusions in Prokaryotes*, Shively, J.M. (ed). Berlin, Germany: Springer, pp. 21–51.

Danza, F., Storelli, N., Roman, S., Lüdin, S., and Tonolla, M. (2017) Dynamic cellular complexity of anoxygenic phototrophic sulfur bacteria in the chemocline of meromictic Lake Cadagno. *PLoS One* **12**: 1–17.

De Yoreo, J.J., Gilbert, P.U., Sommerdijk, N.A., Penn, R.L., Whitelam, S., Joester, D., *et al* (2015) Crystallization by particle attachment in synthetic, biogenic, and geologic environments. *Science (80-)* **349**: aaa6760.

Dehner, C.A., Barton, L., Maurice, P.A., and Dubois, J.L. (2011) Size-dependent bioavailability of hematite (α-Fe_2O_3) nanoparticles to a common aerobic baterium. *Environ Sci Technol* **45**: 977–983.

Deng, X., Dohmae, N., Kaksonen, A.H., and Okamoto, A. (2020) Biogenic Iron Sulfide Nanoparticles to Enable Extracellular Electron Uptake in Sulfate-Reducing Bacteria. *Angew Chemie*, **132**: 6051–6055.

Déniel, M., Errien, N., Daniel, P., Caruso, A., and Lagarde, F. (2019) Current methods to monitor microalgae-nanoparticle interaction and associated effects. *Aquat Toxicol* **217**: 105311.

Dong, H. (2010) Mineral-microbe interactions: a review. *Front Earth Sci China* **4**: 127–147.

Dong, H., Kukkadapu, R.K., Fredrickson, J.K., Zachara, J. M., Kennedy, D.W., and Kostandarithes, H.M. (2003) Microbial reduction of structural Fe(III) in illite and goethite. *Environ Sci Technol* **37**: 1268–1276.

Dufour, S.C., Laurich, J.R., Batstone, R.T., McCuaig, B., Elliott, A., and Poduska, K.M. (2014) Magnetosome-containing bacteria living as symbionts of bivalves. *ISME J* **8**: 2453–2462.

Dupraz, C., Reid, R.P., Braissant, O., Decho, A.W., Norman, R.S., and Visscher, P.T. (2009) Processes of carbonate precipitation in modern microbial mats. *Earth-Science Rev* **96**: 141–162.

Echigo, T., Aruguete, D.M., Murayama, M., and Hochella, M. F. (2012) Influence of size, morphology, surface structure, and aggregation state on reductive dissolution of hematite

nanoparticles with ascorbic acid. *Geochim Cosmochim Acta* **90**: 149–162.

Eskelsen, J.R., Xu, J., Chiu, M., Moon, J.W., Wilkins, B., Graham, D.E., *et al*. (2018) Influence of structural defects on biomineralized ZnS nanoparticle dissolution: an in-situ electron microscopy study. *Environ Sci Technol* **52**: 1139–1149.

Eymard-Vernain, E., Coute, Y., Adrait, A., Rabilloud, T., Sarret, G., and Lelong, C. (2018) The poly-gamma-glutamate of *Bacillus subtilis* interacts specifically with silver nanoparticles. *PLoS One* **13**: 1–19.

Faivre, D., and Schueler, D. (2008) Magnetotactic bacteria and magnetosomes. *Chem Rev* **108**: 4875–4898.

Findlay, A.J., Gartman, A., Macdonald, D.J., Hanson, T.E., Shaw, T.J., and Luther, G.W. (2014) Distribution and size fractionation of elemental sulfur in aqueous environments: the Chesapeake Bay and mid-Atlantic ridge. *Geochim Cosmochim Acta* **142**: 334–348.

Fortin, D., Southam, G., and Beveridge, T.J. (1994) Nickel sulfide, iron-nickel sulfide and iron sulfide precipitation by a newly isolated *Desulfotomaculum* species and its relation to nickel resistance. *FEMS Microbiol Ecol* **14**: 121–132.

Fu, L., Zhou, T., Wang, J., You, L., Lu, Y., Yu, L., and Zhou, S. (2019) NanoFe$_3$O$_4$ as solid electron shuttles to accelerate acetotrophic methanogenesis by *Methanosarcina barkeri*. *Front Microbiol* **10**: 1–13.

Gadd, G.M. (2010) Metals, minerals and microbes: Geomicrobiology and bioremediation. *Microbiology* **156**: 609–643.

Garber, A.I., Nealson, K.H., Okamoto, A., McAllister, S.M., Chan, C.S., Barco, R.A., and Merino, N. (2020) FeGenie: a comprehensive tool for the identification of iron genes and iron gene neighborhoods in genome and metagenome assemblies. *Front Microbiol* **11**: 1–23.

Gartman, A., Findlay, A.J., and Luther, G.W. (2014) Nanoparticulate pyrite and other nanoparticles are a widespread component of hydrothermal vent black smoker emissions. *Chem Geol* **366**: 32–41.

Gil-Allué, C., Tlili, A., Schirmer, K., Gessner, M.O., and Behra, R. (2018) Long-term exposure to silver nanoparticles affects periphyton community structure and function. *Environ Sci Nano* **5**: 1397–1407.

Gilbert, B., Huang, F., Zhang, H., Waychunas, G.A., and Banfield, J.F. (2004) Nanoparticles: strained and stiff. *Science (80-)* **305**: 651–654.

Glass, J.B., and Orphan, V.J. (2012) Trace metal requirements for microbial enzymes involved in the production and consumption of methane and nitrous oxide. *Front Microbiol* **3**: 1–20.

Gleisner, M., Herbert, R.B., and Frogner Kockum, P.C. (2006) Pyrite oxidation by *Acidithiobacillus ferrooxidans* at various concentrations of dissolved oxygen. *Chem Geol* **225**: 16–29.

Graca, B., Zgrundo, A., Zakrzewska, D., Rzodkiewicz, M., and Karczewski, J. (2018) Origin and fate of nanoparticles in marine water - preliminary results. *Chemosphere* **206**: 359–368.

Gray, N., and Head, I. (2014) The family Achromatiaceae. In *The Prokaryotes - Gammaproteobacteria*, Rosenberg, E. (ed). Berlin-Heidelberg: Springer, pp. 1–14.

Gregersen, L.H., Bryant, D.A., and Frigaard, N.-U. (2011) Mechanisms and evolution of oxidative sulfur metabolism in green sulfur bacteria. *Front Microbiol* **2**: 116.

Griffin, S., Masood, M.I., Nasim, M.J., Sarfraz, M., Ebokaiwe, A.P., Schäfer, K.H., *et al*. (2018) Natural nanoparticles: a particular matter inspired by nature. *Antioxidants* **7**.3

Haaijer, S.C.M., Lamers, L.P.M., Smolders, A.J.P., Jetten, M.S.M., and Op den Camp, H.J.M. (2007) Iron sulfide and pyrite as potential electron donors for microbial nitrate reduction in freshwater wetlands. *Geomicrobiol J* **24**: 391–401.

Harouaka, K., Mansor, M., Macalady, J.L., and Fantle, M.S. (2016) Calcium isotopic fractionation in microbially mediated gypsum precipitates. *Geochim Cosmochim Acta* **184**: 114–131.

Harouaka, K., Kubicki, J.D., and Fantle, M.S. (2017) Effect of amino acids on the precipitation kinetics and ca isotopic composition of gypsum. *Geochim Cosmochim Acta* **218**: 343–364.

Hawkings, J.R., Benning, L.G., Raiswell, R., Kaulich, B., Araki, T., Abyaneh, M., *et al*. (2018) Biolabile ferrous iron bearing nanoparticles in glacial sediments. *Earth Planet Sci Lett* **493**: 92–101.

He, H., Zhang, C.-G., Xia, J.-L., Peng, A.-A., Yang, Y., Jiang, H.-C., *et al*. (2009) Investigation of elemental sulfur speciation transformation mediated by *Acidithiobacillus ferrooxidans*. *Curr Microbiol* **58**: 300–307.

Head, I.M., Gray, N.D., Pickup, R.W., and Jones, J.G. (1995) The biogeochemical role of *Achromatium oxaliferum*. In *Organic Geochemistry: Developments and Applications to Energy, Climate, Environment, and Human History*, Grimalt, J.O., and Dorronsoro, C. (eds). A.I.G.O. A: Donostia-San Sebastian, Spain, pp. 895–898.

Hegler, F., Schmidt, C., Schwarz, H., and Kappler, A. (2010) Does a low-pH microenvironment around phototrophic Fe^{II}-oxidizing bacteria prevent cell encrustation by FeIII minerals? *FEMS Microbiol Ecol* **74**: 592–600.

Hirst, C., Andersson, P.S., Shaw, S., Burke, I.T., Kutscher, L., Murphy, M.J., *et al*. (2017) Characterisation of Fe-bearing particles and colloids in the Lena River basin, NE Russia. *Geochim Cosmochim Acta* **213**: 553–573.

Hochella, M.F., Lower, S.K., Maurice, P.A., Penn, R.L., Sahai, N., Sparks, D.L., and Twining, B.S. (2008) Nanominerals, mineral nanoparticles, and earth systems. *Science (80-)* **319**: 1631–1635.

Hochella, M.F., Mogk, D.W., Ranville, J., Allen, I.C., Luther, G.W., Marr, L.C., *et al*. (2019) Natural, incidental, and engineered nanomaterials and their impacts on the earth system. *Science* **80**: 363.

Horstmann, C., Campbell, C., Kim, D.S., and Kim, K. (2019) Transcriptome profile with 20 nm silver nanoparticles in yeast. *FEMS Yeast Res* **19**: 1–15.

Hotze, E.M., Phenrat, T., and Lowry, G.V. (2010) Nanoparticle aggregation: challenges to understanding transport and reactivity in the environment. *J Environ Qual* **39**: 1909–1924.

Houben, G.J., Sitnikova, M.A., and Post, V.E.A. (2017) Terrestrial sedimentary pyrites as a potential source of trace metal release to groundwater—a case study from the Emsland, Germany. *Appl Geochemistry* **76**: 99–111.

Howarth, R., Unz, R.F., Seviour, E.M., Seviour, R.J., Blackall, L.L., Pickup, R.W., *et al*. (1999) Phylogenetic relationships of filamentous sulfur bacteria (*Thiothrix* spp. and Eikelboom type 021 N bacteria) isolated from wastewater-treatment plants and description of *Thiothrix eikelboomii* sp. nov., *Thiothrix unzii* sp. nov., <i>Thi. *Int J Syst Bacteriol* **49**: 1817–1827.

Hu, X., Cook, S., Wang, P., and Hwang, H.m. (2009) In vitro evaluation of cytotoxicity of engineered metal oxide nanoparticles. *Sci Total Environ* **407**: 3070–3072.

Hu, J., Zeng, C., Liu, G., Luo, H., Qu, L., and Zhang, R. (2018) Magnetite nanoparticles accelerate the autotrophic sulfate reduction in biocathode microbial electrolysis cells. *Biochem Eng J* **133**: 96–105.

Huang, F., Gao, W., Gao, S., Meng, L., Zhang, Z., Yan, Y., *et al*. (2017) Morphology evolution of nano-micron pyrite: a review. *J Nanosci Nanotechnol* **17**: 5980–5995.

Huber, C., and Wächtershauser, G. (1998) Peptides by activation of amino acids with CO on (Ni,Fe)S surfaces: implications for the origin of life. *Science (80-)* **281**: 670–672.

Hulkoti, N.I., and Taranath, T.C. (2014) Biosynthesis of nanoparticles using microbes-a review. *Colloids Surfaces B Biointerfaces* **121**: 474–483.

Jiang, X., Hu, J., Lieber, A.M., Jackan, C.S., Biffinger, J.C., Fitzgerald, L.A., *et al*. (2014) Nanoparticle facilitated extracellular electron transfer in microbial fuel cells. *Nano Lett* **14**: 6737–6742.

Johnson, C.A., Freyer, G., Fabisch, M., Caraballo, M.A., Küsel, K., and Hochella, M.F. (2014) Observations and assessment of iron oxide and green rust nanoparticles in metal-polluted mine drainage within a steep redox gradient. *Environ Chem* **11**: 377–391.

Johnston, D.T., Wolfe-Simon, F., Pearson, A., and Knoll, A. H. (2009) Anoxygenic photosynthesis modulated Proterozoic oxygen and sustained Earth's middle age. *Proc Natl Acad Sci U S A* **106**: 16925–16929.

Jørgensen, C.J., Jacobsen, O.S., Elberling, B., and Aamand, J. (2009) Microbial oxidation of pyrite coupled to nitrate reduction in anoxic groundwater sediment. *Environ Sci Technol* **43**: 4851–4857.

Jørgensen, B.B., Findlay, A.J., and Pellerin, A. (2019) The biogeochemical sulfur cycle of marine sediments. *Front Microbiol* **10**: 1–27.

Kallmeyer, J., Pockalny, R., Adhikari, R.R., Smith, D.C., and D'Hondt, S. (2012) Global distribution of microbial abundance and biomass in subseafloor sediment. *Proc Natl Acad Sci U S A* **109**: 16213–16216.

Kang, S., Mauter, M.S., and Elimelech, M. (2009) Microbial cytotoxicity of carbon-based nanomaterials: implications for river water and wastewater effluent. *Environ Sci Technol* **43**: 2648–2653.

Kato, S., and Igarashi, K. (2018) Enhancement of methanogenesis by electric syntrophy with biogenic iron-sulfide minerals. *MicrobiologyOpen* **8**: e00647

Kato, S., Nakamura, R., Kai, F., Watanabe, K., and Hashimoto, K. (2010) Respiratory interactions of soil bacteria with (semi)conductive iron-oxide minerals. *Environ Microbiol* **12**: 3114–3123.

Kato, S., Hashimoto, K., and Watanabe, K. (2012a) Methanogenesis facilitated by electric syntrophy via (semi) conductive iron-oxide minerals. *Environ Microbiol* **14**: 1646–1654.

Kato, S., Hashimoto, K., and Watanabe, K. (2012b) Microbial interspecies electron transfer via electric currents through conductive minerals. *PNAS* **109**: 10042–10046.

Kloepfer, J.A., Mielke, R.E., and Nadeau, J.L. (2005) Uptake of CdSe and CdSe/ZnS quantum dots into bacteria via purine-dependent mechanisms. *Appl Environ Microbiol* **71**: 2548–2557.

Kostka, J.E., Dalton, D.D., Skelton, H., Dollhopf, S., and Stucki, J.W. (2002) Growth of iron (III)-reducing bacteria on clay minerals as the sole electron acceptor and comparison of growth yields on a variety of oxidized iron forms. *Appl Environ Microbiol* **68**: 6256–6262.

Kreutzmann, A.C., and Schulz-Vogt, H.N. (2016) Oxidation of molecular hydrogen by a chemolithoautotrophic *Beggiatoa* strain. *Appl Environ Microbiol* **82**: 2527–2536.

Labrado, A.L., Brunner, B., Bernasconi, S.M., and Peckmann, J. (2019) Formation of large native sulfur deposits does not require molecular oxygen. *Front Microbiol* **10**: 1–26.

Lagarde, F., Olivier, O., Zanella, M., Daniel, P., Hiard, S., and Caruso, A. (2016) Microplastic interactions with freshwater microalgae: hetero-aggregation and changes in plastic density appear strongly dependent on polymer type. *Environ Pollut* **215**: 331–339.

Lazo, D.E., Dyer, L.G., and Alorro, R.D. (2017) Silicate, phosphate and carbonate mineral dissolution behaviour in the presence of organic acids: a review. *Miner Eng* **100**: 115–123.

Lee, S., Bi, X., Reed, R.B., Ranville, J.F., Herckes, P., and Westerhoff, P. (2014) Nanoparticle size detection limits by single particle ICP-MS for 40 elements. *Environ Sci Technol* **48**: 10291–10300.

Lefevre, C.T., and Bazylinski, D.A. (2013) Ecology, diversity, and evolution of magnetotactic bacteria. *Microbiol Mol Biol Rev* **77**: 497–526.

Legg, B.A., Zhu, M., Comolli, L.R., Gilbert, B., and Banfield, J.F. (2014a) Determination of the three-dimensional structure of ferrihydrite nanoparticle aggregates. *Langmuir* **30**: 9931–9940.

Legg, B.A., Zhu, M., Comolli, L.R., Gilbert, B., and Banfield, J.F. (2014b) Impacts of ionic strength on three-dimensional nanoparticle aggregate structure and consequences for environmental transport and deposition. *Environ Sci Technol* **48**: 13703–13710.

Levar, C.E., Hoffman, C.L., Dunshee, A.J., Toner, B.M., and Bond, D.R. (2017) Redox potential as a master variable controlling pathways of metal reduction by *Geobacter sulfurreducens*. *ISME J* **11**: 741–752.

Li, G., Sun, J., Hou, W., Jiang, S., Huang, Y., and Geng, J. (2016) Three-dimensional porous carbon composites containing high sulfur nanoparticle content for high-performance lithium-sulfur batteries. *Nat Commun* **7**: 1–10.

Li, X., Qin, F., Chen, X., Sheng, A., Wang, Z., and Liu, J. (2019) Dissolution behavior of isolated and aggregated hematite particles revealed by in situ liquid cell transmission electron microscopy. *Environ Sci Technol* **53**: 2416–2425.

Lin, W., Pan, Y., and Bazylinski, D.A. (2017) Diversity and ecology of and biomineralization by magnetotactic bacteria. *Environ Microbiol Rep* **9**: 345–356.

Liu, J., Aruguete, D.M., Murayama, M., and Hochella, M.F., Jr. (2009) Influence of size and aggregation on the reactivity of an environmentally and industrially relevant nanomaterial (PbS). *Environ Sci Technol* **43**: 8178–8183.

Liu, F., Rotaru, A.E., Shrestha, P.M., Malvankar, N.S., Nevin, K.P., and Lovley, D.R. (2012) Promoting direct interspecies electron transfer with activated carbon. *Energ Environ Sci* **5**: 8982–8989.

Liu, J., Pearce, C.I., Shi, L., Wang, Z., Shi, Z., Arenholz, E., and Rosso, K.M. (2016) Particle size effect and the mechanism of hematite reduction by the outer membrane cytochrome OmcA of *Shewanella oneidensis* MR-1. *Geochim Cosmochim Acta* **193**: 160–175.

Mansor, M., Hamilton, T.L., Fantle, M.S., and Macalady, J.L. (2015) Metabolic diversity and ecological niches of *Achromatium* populations revealed with single-cell genomic sequencing. *Front Microbiol* **6**: 1–14.

Mansor, M., Berti, D., Hochella, M.F., Jr., Murayama, M., and Xu, J. (2019a) Phase, morphology, elemental composition and formation mechanisms of biogenic and abiogenic Fe-cu-sulfide nanoparticles: a comparative study on their occurrences under anoxic conditions. *Am Mineral* **104**: 703–717.

Mansor, M., Winkler, C., Hochella, M.F., Jr., and Xu, J. (2019b) Nanoparticulate nickel-hosting phases in sulfidic environments: effects of ferrous iron and bacterial presence on mineral formation mechanism and solid-phase nickel distribution. *Front Earth Sci - Earth Planet Mater* **7**: 151.

Mansor, M., Cantando, E., Wang, Y., Hernandez-Viezcas, J. A., Gardea-Torresdey, J.L., Hochella, M.F., Jr., and Xu, J. (2020) Insights into the biogeochemical cycling of cobalt: precipitation and transformation of cobalt sulfide nanoparticles under low-temperature aqueous conditions. *Environ Sci Technol* **54**: 5598–5607.

Marnocha, C.L., Sabanayagam, C.R., Modla, S., Powell, D. H., Henri, P.A., Steele, A.S., *et al.* (2019) Insights into the mineralogy and surface chemistry of extracellular biogenic S^0 globules produced by *Chlorobaculum tepidum*. *Front Microbiol* **10**: 1–11.

Mehta, N., Benzerara, K., Kocar, B.D., and Chapon, V. (2019) Sequestration of radionuclides radium-226 and strontium-90 by cyanobacteria forming intracellular calcium carbonates. *Environ Sci Technol* **53**: 12639–12647.

Melton, E.D., Swanner, E.D., Behrens, S., Schmidt, C., and Kappler, A. (2014) The interplay of microbially mediated and abiotic reactions in the biogeochemical Fe cycle. *Nat Rev Microbiol* **12**: 797–808.

Metch, J.W., Burrows, N.D., Murphy, C.J., Pruden, A., and Vikesland, P.J. (2018) Metagenomic analysis of microbial communities yields insight into impacts of nanoparticle design. *Nat Nanotechnol* **13**: 253–259.

Miot, J., Benzerara, K., Morin, G., Kappler, A., Bernard, S., Obst, M., *et al.* (2009) Iron biomineralization by anaerobic neutrophilic iron-oxidizing bacteria. *Geochim Cosmochim Acta* **73**: 696–711.

Miot, J., Benzerara, K., and Kappler, A. (2014) Investigating microbe-mineral interactions: recent advances in X-ray and electron microscopy and redox-sensitive methods. *Annu Rev Earth Planet Sci* **42**: 271–289.

Miot, J., Remusat, L., Duprat, E., Gonzalez, A., Pont, S., and Poinsot, M. (2015) Fe biomineralization mirrors individual metabolic activity in a nitrate-dependent Fe(II)-oxidizer. *Front Microbiol* **6**: 1–13.

Misra, S.K., Dybowska, A., Berhanu, D., Luoma, S.N., and Valsami-Jones, E. (2012) The complexity of nanoparticle dissolution and its importance in nanotoxicological studies. *Sci Total Environ* **438**: 225–232.

Monrás, J.P., Collao, B., Molina-Quiroz, R.C., Pradenas, G. A., Saona, L.A., Durán-Toro, V., *et al.* (2014) Microarray analysis of the *Escherichia coli* response to CdTe-GSH quantum dots: understanding the bacterial toxicity of semiconductor nanoparticles. *BMC Genomics* **15**: 1–13.

Monteil, C.L., Vallenet, D., Menguy, N., Benzerara, K., Barbe, V., Fouteau, S., *et al.* (2019) Ectosymbiotic bacteria at the origin of magnetoreception in a marine protist. *Nat Microbiol* **4**: 1088–1095.

Moreau, J.W., Webb, R.I., and Banfield, J.F. (2004) Ultrastructure, aggregation-state, and crystal growth of biogenic nanocrystalline sphalerite and wurtzite. *Am Mineral* **89**: 950–960.

Natan, E., and Vortman, Y. (2017) The symbiotic magnetic-sensing hypothesis: do magnetotactic bacteria underlie the magnetic sensing capability of animals? *Mov Ecol* **5**: 1–5.

Nims, C., Cron, B., Wetherington, M., Macalady, J., and Cosmidis, J. (2019) Low frequency Raman spectroscopy for micron-scale and *in vivo* characterization of elemental sulfur in microbial samples. *Sci Rep* **9**: 1–12.

Novotnik, B., Zorz, J., Bryant, S., and Strous, M. (2019) The effect of dissimilatory manganese reduction on lactate fermentation and microbial community assembly. *Front Microbiol* **10**: 1–15.

Pal, S., Tak, Y.K., and Song, J.M. (2007) Does the antibacterial activity of silver nanoparticles depend on the shape of the nanoparticle? A study of the gram-negative bacterium *Escherichia coli*. *Appl Environ Microbiol* **73**: 1712–1720.

Pentráková, L., Su, K., Pentrák, M., and Stucki, J.W. (2013) A review of microbial redox interactions with structural Fe in clay minerals. *Clay Miner* **48**: 543–560.

Percak-Dennett, E., He, S., Converse, B., Konishi, H., Xu, H., Corcoran, A., *et al.* (2017) Microbial acceleration of aerobic pyrite oxidation at circumneutral pH. *Geobiology* **15**: 690–703.

Picard, A., Gartman, A., and Girguis, P.R. (2016) What do we really know about the role of microorganisms in iron sulfide mineral formation? *Front Earth Sci* **4**: 1–10.

Picard, A., Gartman, A., Clarke, D.R., and Girguis, P.R. (2018) Sulfate-reducing bacteria influence the nucleation and growth of mackinawite and greigite. *Geochim Cosmochim Acta* **220**: 367–384.

Posth, N.R., Canfield, D.E., and Kappler, A. (2014) Biogenic Fe(III) minerals: from formation to diagenesis and preservation in the rock record. *Earth-Science Rev* **135**: 103–121.

Priester, J.H., Stoimenov, P.K., Mielke, R.E., Webb, S.M., Ehrhardt, C., Zhang, J.P., *et al.* (2009) Effects of soluble cadmium salts versus CdSe quantum dots on the growth

of planktonic *Pseudomonas aeruginosa*. *Environ Sci Technol* **43**: 2589–2594.

Pu, J., Feng, C., Liu, Y., Li, R., Kong, Z., Chen, N., *et al*. (2014) Pyrite-based autotrophic denitrification for remediation of nitrate contaminated groundwater. *Bioresour Technol* **173**: 117–123.

Raven, J.A., Evans, M.C., and Korb, R.E. (1999) The role of trace metals in photosynthetic electron transport in O_2-evolving organisms. *Photosynth Res* **60**: 111–150.

Revel, M., Châtel, A., and Mouneyrac, C. (2017) Omics tools: new challenges in aquatic nanotoxicology? *Aquat Toxicol* **193**: 72–85.

Rickard, D., and Luther, G.W. (2007) Chemistry of iron sulfides. *Chem Rev* **107**: 514–562.

Rimstidt, D.D., and Vaughan, D.J. (2003) Pyrite oxidation: a state-of-the-art assessment of the reaction mechanism. *Geochim Cosmochim Acta* **67**: 873–880.

Robie, R.A., and Bethke, P. (1966) Molar volumes and densities of minerals. *Handb Phys Constants, Geol Soc Am Mem* **97**: 371–383.

Rotaru, A.-E., Calabrese, F., Stryhanyuk, H., Musat, F., Shrestha, P.M., Weber, H.S., *et al*. (2018) Conductive particles enable syntrophic acetate oxidation between *Geobacter* and *Methanosarcina* from coastal sediments. *MBio* **9**: e00226–e00218.

Rotaru, A.-E., Posth, N.R., Löscher, C., Miracle, M., Vicente, E., Cox, R.P., *et al*. (2019) Interspecies interactions mediated by conductive minerals in the sediments of the iron rich meromictic Lake La Cruz, Spain. *Limnetica* **38**: 21–40.

Saini, G., and Chan, C.S. (2013) Near-neutral surface charge and hydrophilicity prevent mineral encrustation of Fe-oxidizing micro-organisms. *Geobiology* **11**: 191–200.

Sakimoto, K.K., Wong, A.B., and Yang, P. (2016) Self-photosensitization of nonphotosynthetic bacteria for solar-to-chemical production. *Science (80-)* **351**: 74–77.

Salman, V., Amann, R., Girnth, A.C., Polerecky, L., Bailey, J. V., Høgslund, S., *et al*. (2011) A single-cell sequencing approach to the classification of large, vacuolated sulfur bacteria. *Syst Appl Microbiol* **34**: 243–259.

Schacht, V.J., Neumann, L.V., Sandhi, S.K., Chen, L., Henning, T., Klar, P.J., *et al*. (2012) Effects of silver nanoparticles on microbial growth dynamics. *J Appl Microbiol* **114**: 25–35.

Schindler, M., Mantha, H., and Hochella, M.F. (2019) The formation of spinel-group minerals in contaminated soils: the sequestration of metal(loid)s by unexpected incidental nanoparticles. *Geochem Trans* **20**: 1–12.

Schippers, A., and Jorgensen, B.B. (2002) Biogeochemistry of pyrite and iron sulfide oxidation in marine sediments. *Geochim Cosmochim Acta* **66**: 85–92.

Schulz, H.N., Teske, A.J., and BB, O. (1999) Dense populations of a giant sulfur bacterium in Namibian shelf sediments. *Science (80-)* **284**: 493–495.

Shankar, S., Jaiswal, L., and Rhim, J.-W. (2020) New insight into sulfur nanoparticles: synthesis and applications. *Crit Rev Environ Sci Technol*: 1–28. https://doi.org/10.1080/10643389.2020.1780880.

Shao, P.P., Comolli, L.R., and Bernier-Latmani, R. (2014) Membrane vesicles as a novel strategy for shedding encrusted cell surfaces. *Minerals* **4**: 74–88.

Sharma, V.K., Siskova, K.M., Zboril, R., and Gardea-Torresdey, J.L. (2014) Organic-coated silver nanoparticles in biological and environmental conditions: fate, stability and toxicity. *Adv Colloid Interface Sci* **204**: 15–34.

Sharma, V.K., Filip, J., Zboril, R., and Varma, R.S. (2015) Natural inorganic nanoparticles – formation, fate, and toxicity in the environment. *Chem Soc Rev* **44**: 8410–8423.

Shi, L., Dong, H., Reguera, G., Beyenal, H., Lu, A., Liu, J., *et al*. (2016) Extracellular electron transfer mechanisms between microorganisms and minerals. *Nat Rev Microbiol* **14**: 651–662.

Shrihari, R.K., Modak, J.M., Kumar, R.K., and Gandhi, K.S. (1995) Dissolution of particles of pyrite mineral by direct attachment of *Thiobacillus ferrooxidans Hydrometallurgy*. **38**: 175–187.

Simon, D.F., Domingos, R.F., Hauser, C., Hutchins, C.M., Zerges, W., and Wilkinson, K.J. (2013) Transcriptome sequencing (RNA-seq) analysis of the effects of metal nanoparticle exposure on the transcriptome of *Chlamydomonas reinhardtii*. *Appl Environ Microbiol* **79**: 4774–4785.

Singh, S. (2019) Zinc oxide nanoparticles impacts: cytotoxicity, genotoxicity, developmental toxicity, and neurotoxicity. *Toxicol Mech Methods* **29**: 300–311.

Singh, N., Paknikar, K.M., and Rajwade, J. (2019) RNA-sequencing reveals a multitude of effects of silver nanoparticles on *Pseudomonas aeruginosa* biofilms. *Environ Sci Nano* **6**: 1812–1828.

Stanley, W., and Southam, G. (2018) The effect of gram-positive (*Desulfosporosinus orientis*) and gram-negative (*Desulfovibrio desulfuricans*) sulfate-reducing bacteria on iron sulfide mineral precipitation. *Can J Microbiol* **64**: 629–637.

Stauber, R.H., Siemer, S., Becker, S., Ding, G.B., Strieth, S., and Knauer, S.K. (2018) Small meets smaller: effects of nanomaterials on microbial biology, pathology, and ecology. *ACS Nano* **12**: 6351–6359.

Steudel, R. (1989) On the nature of the "elemental sulfur" (S°) produced by sulfur-oxidizing bacteria—a model for S° globules. In *Biology of Autotrophic Bacteria*, Schlegel, H. G., and Bowien, B. (eds). Madison: Science Technology Publications, pp. 289–303.

Tang, R., Wang, L., and Nancollas, G.H. (2004) Size-effects in the dissolution of hydroxyapatite: an understanding of biological demineralization. *J Mater Chem* **14**: 2341–2346.

Tang, J., Zhuang, L., Ma, J., Tang, Z., Yu, Z., and Zhou, S. (2016) Secondary mineralization of ferrihydrite affects microbial methanogenesis in *Geobacter-Methanosarcina* cocultures. *Appl Environ Microbiol* **82**: 5869–5877.

Tepe, N., and Bau, M. (2014) Importance of nanoparticles and colloids from volcanic ash for riverine transport of trace elements to the ocean: evidence from glacial-fed rivers after the 2010 eruption of Eyjafjallajökull volcano, Iceland. *Sci Total Environ* **488–489**: 243–251.

Tepe, N., and Bau, M. (2015) Distribution of rare earth elements and other high field strength elements in glacial meltwaters and sediments from the western Greenland ice sheet: evidence for different sources of particles and nanoparticles. *Chem Geol* **412**: 59–68.

Thiel, J., Byrne, J.M., Kappler, A., Schink, B., and Pester, M. (2019) Pyrite formation from FeS and H_2S is mediated

through microbial redox activity. *Proc Natl Acad Sci* **116**: 6897–6902.

Torrentó, C., Cama, J., Urmeneta, J., Otero, N., and Soler, A. (2010) Denitrification of groundwater with pyrite and *Thiobacillus denitrificans*. *Chem Geol* **278**: 80–91.

Tromans, D., and Meech, J.A. (2002) Fracture toughness and surface energies of covalent minerals: theoretical estimates. *Miner Eng* **15**: 1027–1041.

Vaclavkova, S., Schultz-Jensen, N., Jacobsen, O.S., Elberling, B., and Aamand, J. (2015) Nitrate-controlled anaerobic oxidation of pyrite by *Thiobacillus* cultures. *Geomicrobiol J* **32**: 412–419.

Vargas, G., Cypriano, J., Correa, T., Leão, P., Bazylinski, D. A., and Abreu, F. (2018) Applications of magnetotactic bacteria, magnetosomes and magnetosome crystals in biotechnology and nanotechnology: mini-review. *Molecules* **23**: 2438.

Vorhies, J.S., and Gaines, R.R. (2009) Microbial dissolution of clay minerals as a source of iron and silica in marine sediments. *Nat Geosci* **2**: 221–225.

Wagner, S., Gondikas, A., Neubauer, E., Hofmann, T., and Von Der Kammer, F. (2014) Spot the difference: engineered and natural nanoparticles in the environment-release, behavior, and fate. *Angew Chemie - Int Ed* **53**: 12398–12419.

Wang, B., Zeng, C., Chu, K.H., Wu, D., Yip, H.Y., and Ye, L. (2017) Enhanced biological hydrogen production from *Escherichia coli* with surface precipitated cadmium sulfide nanoparticles. *Adv Energy Mater* **7**: 1700611.

Westmeier, D., Posselt, G., Hahlbrock, A., Bartfeld, S., Wessler, S., and Stauber, R.H. (2018) Nanoparticle binding attenuates the pathobiology of gastric cancer-associated *Helicobacter pylori*. *Nanoscale* **10**: 1453–1463.

Wright, M.H., Farooqui, S.M., White, A.R., and Greene, A.C. (2016) Production of manganese oxide nanoparticles by *Shewanella* species. *Appl Environ Microbiol* **82**: 5402–5409.

Xu, J., Campbell, J.M., Zhang, N., Hickey, W.J., and Sahai, N. (2012) Did mineral surface chemistry and toxicity contribute to evolution of microbial extracellular polymeric substances? *Astrobiology* **12**: 785–798.

Xu, J., Murayama, M., Roco, C.M., Veeramani, H., Michel, F. M., Rimstidt, J.D., *et al* (2016) Highly-defective nano-crystals of ZnS formed via dissimilatory bacterial sulfate reduction: a comparative study with their abiogenic analogues. *Geochim Cosmochim Acta* **180**: 1–14.

Yamada, C., Kato, S., Ueno, Y., Ishii, M., and Igarashi, Y. (2015) Conductive iron oxides accelerate thermophilic methanogenesis from acetate and propionate. *J Biosci Bioeng* **119**: 678–682.

Yan, B., Wrenn, B.A., Basak, S., Biswas, P., and Giammar, D.E. (2008) Microbial reduction of Fe(III) in hematite nanoparticles by *Geobacter sulfurreducens*. *Environ Sci Technol* **42**: 6526–6531.

Yan, R., Kappler, A., Muehe, E.M., and Knorr, K. (2018) Effect of reduced sulfur species on chemolithoautotrophic pyrite oxidation with nitrate. *Geomicrobiol J* **0**: 1–10.

Yang, Z., Sun, T., Subdiaga, E., Obst, M., Haderlein, S.B., Maisch, M., *et al.* (2020) Aggregation-dependent electron transfer via redox-active biochar particles stimulate microbial ferrihydrite reduction. *Sci Total Environ* **703**: 135515.

You, Y., Zheng, S., Zang, H., Liu, Feng, Liu Fanghua, and Liu, J. (2018) Stimulatory effect of magnetite on the syntrophic metabolism of *Geobacter* co-cultures: influences of surface coating. *Geochim Cosmochim Acta*, **256**, 82–96.

Zeng, Q., Huang, L., Ma, J., Zhu, Z., He, C., Shi, Q., *et al.* (2020) Bio-reduction of ferrihydrite-montmorillonite-organic matter complexes: effect of montmorillonite and fate of organic matter. *Geochim Cosmochim Acta* **276**: 327–344.

Zhuang, L., Xu, J., Tang, J., and Zhou, S. (2015) Effect of ferrihydrite biomineralization on methanogenesis in an anaerobic incubation from paddy soil. *J Geophys Res Biogeo* **120**: 876–886.

Zhuang, L., Ma, J., Yu, Z., Wang, Y., and Tang, J. (2018) Magnetite accelerates syntrophic acetate oxidation in methanogenic systems with high ammonia concentrations. *J Microbial Biotechnol* **11**: 710–720.